Surface Review and Letters, Vol. 3, No. 2 (1996) 1295–1303
© World Scientific Publishing Company

AB-INITIO STUDIES OF DIFFUSION AND GROWTH PHENOMENA ON SEMICONDUCTOR SURFACES

EFTHIMIOS KAXIRAS
Department of Physics and Division of Applied Sciences,
Harvard University, Cambridge, Massachusetts 02138, USA

Received 31 October 1995

We discuss the application of *ab-initio* quantum-mechanical calculations, based on pseudopotential local-density-functional theory, to diffusion and growth phenomena on semiconductor surfaces. We examine in detail two specific examples: adatom diffusion on the Ge(111)c(2×8) reconstructed surface and surfactant-mediated homoepitaxial growth on Si substrates. In these examples, the combination of results from first-principles calculations and simple simulations helps elucidate complex dynamical phenomena. We also make predictions on the feasibility of using hydrogen as a surfactant on Si substrates, by drawing analogies between the chemical behavior of group-V or group-VI adsorbates and Si–H complexes.

1. Introduction

In the last two decades, first-principles calculations based on density functional theory with the local density approximation,[1–3] and using pseudopotentials to represent the atomic cores,[4] have proven a versatile and powerful tool for studying various properties of solids. Typical applications of the theory include determination through total-energy comparisons of the equilibrium properties of bulk, surface and defect structures. More recently, this theory has even been applied to the study of complex surface reconstructions with very large unit cells.[5] While these accomplishments are impressive, a wide class of dynamical phenomena, such as diffusion and growth, pose an even bigger challenge to the theory. In kinetically controlled processes, it is desirable to obtain accurate estimates of activation free energies. Experience in calculating activation free energies is still limited, mainly for two reasons. First, it is often quite difficult to determine the structure of a saddle-point configuration that corresponds to the activation-energy barrier, especially in a system with a large number of degrees of freedom; a few *ab-initio* calculations of activation-energy barriers on semiconductor surfaces have been reported to date.[6–10] Second, even if the activation-energy barrier can be determined accurately, it is computationally very demanding to calculate the entropy contribution in order to obtain the activation free energy.[11]

There is significant computational cost in performing first-principles calculations for systems of size larger than a few tens of atoms, because the problem of interacting electrons and ions is being solved within a quantum-mechanical framework, where the electronic degrees of freedom are treated explicitly and self-consistently. Calculations involving more than a few tens of atoms can be performed only on supercomputers, and rely on efficient use of vectorization and parallelization techniques to make the computation feasible.[5] Nevertheless, there are important advantages in performing these computationally demanding calculations: in cases where experiment produces unexpected results that are not easily rationalized by simple arguments, these calculations can provide reliable comparisons that allow a successful resolution of the puzzle. Moreover, first-principles calculations apply to a wide variety of physical systems and are not restricted to a particular model material, such as Si; this makes it possible to examine realistic structures that contain various types of atoms, and allows direct comparison to relevant experiments.

In this paper we discuss our recent work in applying pseudopotential local-density-functional calculations to obtain activation free energies for diffusion and growth phenomena on semiconductor surfaces. We also discuss some simple Monte Carlo simulations, which are based on the results of the first-principles calculations, and are of crucial importance in making contact with experimental results.

2. Adatom Exchange on a Reconstructed Surface

The first example concerns the experimentally observed very slow adatom diffusion rate on the Ge(111)c(2×8) reconstructed surface.[12] Diffusion on this surface takes place through exchange of adatom positions. The equilibrium adatom concentration is dictated by the stable surface reconstruction: it corresponds to one adatom per four surface dangling bonds, three of which are saturated by the presence of the adatom while the fourth is left unsaturated. The atom with the unsaturated dangling bond is called a "rest atom." This arrangement of atoms significantly reduces the density of dangling bonds on the surface, without introducing excessive strain. At the temperature range where diffusion is measured experimentally, the reconstruction pattern remains intact, so that after exchange the adatoms reside on regular sites of the reconstructed surface. In the diffusion experiments, a small number (5–10%) of Ge adatoms were substituted by Pb adatoms, which serve as tracers because they appear as slightly brighter spots in the scanning-tunneling-microscope (STM) images. From the chemical point of view, the Pb adatoms behave very similarly to the Ge adatoms, saturating three substrate dangling bonds each.

The diffusion constant is given by

$$D = f\nu l^2 \exp\left(\frac{S}{k_B}\right) \exp\left(-\frac{\varepsilon_d}{k_B T}\right), \qquad (1)$$

where ν is the attempt frequency, l is the hopping length, S is the entropy associated with the diffusion process, and ε_d is the activation-energy barrier. f is a geometric factor, which for exchange is equal to 1. D was measured by comparing STM images taken at regular time intervals and counting the number of adatom exchanges between successive images, as a function of the temperature.[12] The resulting

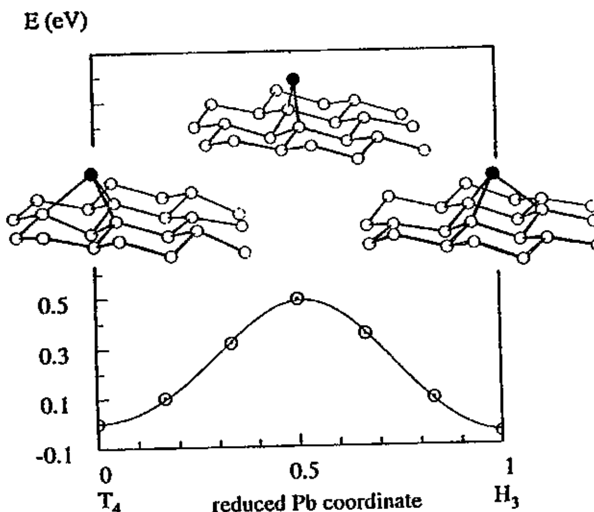

Fig. 1. The calculated energy for hopping of a single Pb adatom (shaded) from the T_4 position, through the intermediate bridge position, to the H_3 position. The structure of the three configurations is shown in the insets.

Arrhenius plot provides a measurement of the activation energy and the pre-exponential factor. The activation energy is $\varepsilon_d = 0.54 \pm 0.03$ eV, a typical figure for such processes [very similar, for example, to the diffusion barrier for motion of an adatom on the Si(100) surface[13]]. Surprisingly, the measured value of the pre-exponential factor $D_0 = \nu l^2 \exp(S/k_B) = 10^{-9}$ cm^2 sec^{-1} is approximately six orders of magnitude lower than would be expected, if typical estimates were to be used for the hopping length l (of order a few Å) and the attempt frequency ν (of order 10^{13} sec^{-1}); these values give a D_0 of order 10^{-3} cm^2 sec^{-1} (entropy effects are neglected in this simple estimate).

For the Ge(111)c(2 × 8) reconstructed surface, it is possible to identify the elementary hop of individual adatoms that has the lowest activation energy. This involves a move from the T_4 equilibrium position to the H_3 metastable position through the bridge position, as illustrated in the insets of Fig. 1. Diffusion through this process involves the breaking of a single covalent bond, which is reformed once the adatom has moved from the T_4 to the H_3 position. Any other motion that breaks more than one covalent bond will have a higher activation energy. Notice that the presence of a rest atom in the immediate neighborhood of the adatom is needed to make the T_4-to-H_3 motion possible. The simplicity

of the path, which can be described by a single coordinate (the position of the adatom along a line joining the equilibrium, through the saddle point, to the metastable site) facilitates the calculation of the energy barrier. All other atoms are fully relaxed during this motion. Our first-principles calculations show that the activation energy for this simple hop, for a Pb adatom that has replaced a Ge adatom on the reconstructed layer, is 0.56 ± 0.05 eV (see Fig. 1). This is very close to the experimentally measured value. The activation energy for hopping of Ge adatoms through the same path is very similar, namely 0.58 ± 0.05 eV. Both results are within error bars[14] of the experimental number. For Ge adatoms the H_3 position is higher in energy than the T_4 position, whereas for the Pb adatom the two positions are energetically equivalent, within the accuracy of the calculations (see Fig. 1). These results establish that the motion of adatoms involves hopping between T_4 and H_3 sites, since other mechanisms involving more severe distortions of the surface layer would have higher activation energy. What remains to be explained is the observed very slow rate of exchange between adatom sites that leads to adatom diffusion. This slow rate could in principle be due to an unusually low attempt frequency or to an entropy term that effectively reduces the hopping rate (i.e. a negative entropy for diffusion which would be a rather unusual situation).

The attempt frequency and entropy factor can be estimated using first-principles total-energy calculations and Vineyard's transition-state theory.[15] In this approach, the rate of diffusion is given as the ratio of two Boltzmann integrals:

$$\Gamma = \left(\frac{k_B T}{2\pi m}\right)^{\frac{1}{2}} \frac{\int dA \exp[-(E(A) - \varepsilon_d)/k_B T]}{\int d\Omega \exp[-E(\Omega)/k_B T]} . \quad (2)$$

In the above equation, the numerator is an integral over the saddle-point surface, i.e. a $(3N-1)$-dimensional hypersurface (where N is the total number of particles in the system) that passes through the saddle-point configuration and is locally orthogonal to constant energy contours; the denominator is an integral over the $3N$-dimensional space around the equilibrium configuration of the system; ε_d is the activation energy for diffusion and m is a reduced mass corresponding to the coordinate that describes the diffusion path. From this expression, the attempt frequency can be obtained as the average of the energy curvature around the equilibrium configuration, and the entropy as the logarithm of the ratio of the two Boltzmann integrals, once they have been cast into dimensionless form.[15] Using this formalism, our calculations show that the attempt frequency for individual hops is 2×10^{11} sec^{-1}, reasonably close to the simple estimate mentioned above, and the entropy of diffusion is $1.5k_B$, which would tend to *enhance* rather than reduce the hopping rate. If we assume that the individual T_4-to-H_3 hops contain all the information necessary for

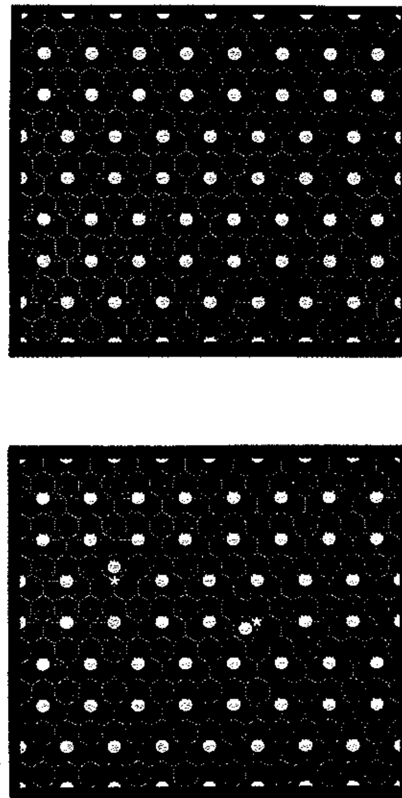

Fig. 2. Illustration of the constraints imposed on the motion of a single adatom by the presence of its neighbors. In the fully ordered surface, which has a c(2×8) reconstruction (upper panel), all adatoms are at equilibrium T_4 positions. Each adatom (yellow dot) possesses an exclusion zone indicated by the short red lines emanating from the position of the adatom: this zone denotes other T_4 or H_3 neighboring positions that cannot be occupied because of the presence of a given adatom. The exclusion zones cannot overlap, because that would violate the bonding requirements of individual adatoms. The lower panel shows two adatoms that have moved to H_3 positions, with the emptied T_4 positions marked by white asterisks. When an adatom moves, it carries along its exclusion zone. Due to the presence of the exclusion zones of neighboring adatoms, no further motion is possible after the first single hop, unless an orchestrated event occurs.

explaining diffusion, we can use the distance between the T_4 and H_3 sites as the hopping length l = 2.3 Å, and the calculated values for the attempt frequency and the entropy of diffusion, to obtain a pre-exponential factor of $D_0 = 0.5 \times 10^{-3}$ cm^2 sec^{-1}. Comparing this value to the experimentally measured value of 10^{-9} cm^2 sec^{-1}, we conclude that the discrepancy of six orders of magnitude cannot be explained by the single T_4-to-H_3 hopping process.

In order to explain this apparent discrepancy, we have proposed that the ordered surface reconstruction, together with the restriction that adatom motion involves the minimal amount of bond breaking, can lead to adatom exchanges only through very complicated sequential displacement of neighboring adatoms.[7] To motivate this idea, we show in Fig. 2 a fully ordered reconstruction (upper panel) and one in which a couple of adatoms have moved from equilibrium T_4 positions to metastable H_3 positions (lower panel). Once an adatom has performed such a single hop starting from the equilibrium position, its further movement is prohibited because its neighbors block all other available sites in the vicinity of the moved adatom, except for the original position. A move back to that position would not lead to an exchange event and cannot be counted as part of the diffusion process. The blocking of sites due to the presence of neighbors is indicated in Fig. 2 by short red lines emanating from each occupied position (yellow dot) to the adjacent blocked sites. These lines form an "exclusion zone" around each adatom. When adatoms move, they carry along their exclusion zones, as shown for the two displaced adatoms in the lower panel of Fig. 2. The exclusion zones cannot overlap, because this would violate the bonding requirements of each adatom. Thus, if and only if at exactly the right moment the neighbors of a displaced adatom move out of its way, can this adatom migrate further and eventually exchange positions with one of its neighboring adatoms.

In order to extract quantitative results for the diffusion rate under these restrictions, we have studied this process with a Monte Carlo (MC) simulation where adatoms move between T_4 and H_3 sites carrying along their exclusion zones. Exchange between adatom positions can occur only through a very complicated sequence of T_4-to-H_3 and H_3-to-T_4 moves. One such event, in which five adatoms have changed positions, with the help of several other adatoms which happened to move in the right way at the right moment, is shown in Fig. 3. We have performed simulations in which many such events

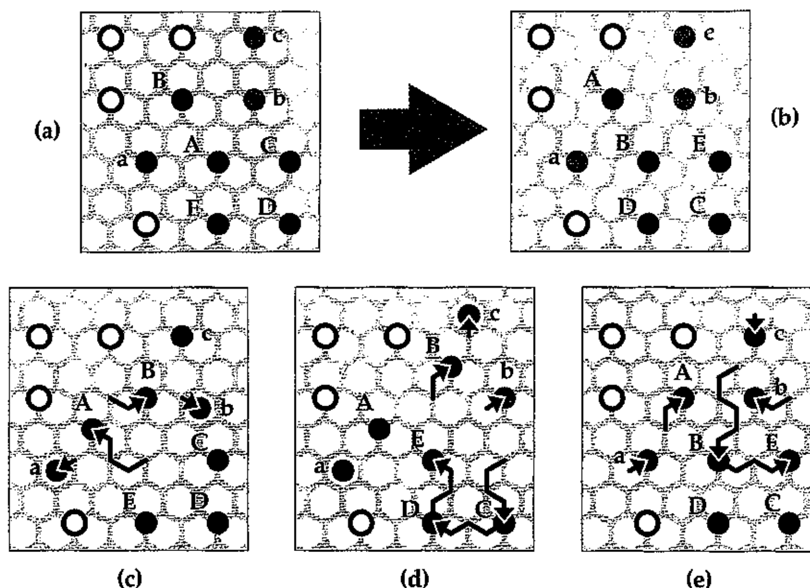

Fig. 3. Example of an orchestrated exchange event, involving the displacement of five adatoms (labeled A, B, C, D, E and marked by black dots), which change positions between (a) the initial and (b) the final configurations (top two panels). The movement of three other adatoms (labeled a, b, c and marked by gray dots) was essential in allowing the exchange of positions between adatoms A, B, C, D, E; adatoms a, b, c end up in their original positions. The adatoms not involved in the event are shown as open circles. Each part of the event consists of sequential T_4-to-H_3 or H_3-to-T_4 hops (denoted by arrows), as shown in the three lower panels, (c), (d), (e), where the orchestrated exchange event is analyzed in terms of the individual hops that constitute it.

of various degrees of complexity were observed. We refer to these events as "orchestrated exchanges," due to the highly complicated nature of the motion. The results show that while an orchestrated adatom exchange involves order $\delta_\tau = 10^2$ MC moves and includes displacement of several (2–10) adatoms, the interval between successive exchanges is on average equal to $\Delta\tau = 10^6$ MC moves. Note that since each move in the simulation represents an elementary T_4-to-H_3 hop (or the reverse), and an exchange event comprises many *sequential* elementary hops, the activation energy is that of a single hop. The rarity of the complicated events that lead to adatom exchange through a sequence of elementary hops explains the effective retardation of the diffusion rate. The MC simulations provide a measure of this retardation, namely the factor $(\Delta\tau)^{-1} = 10^{-6}$, which brings the theory into excellent agreement with experiment.

3. Surfactant-Mediated Epitaxial Growth

We discuss next a different situation where first-principles results provide comparisons essential to deciphering and *predicting* the behavior of a complex system. Copel *et al.*[16] first reported that the use of surfactants in heteroepitaxial growth of semiconductors could alter qualitatively the mode of growth: using As as a surfactant, these authors were able to grow epitaxial layers of Ge on a Si(100) substrate for a thickness an-order-of-magnitude larger than in the absence of the surfactant. More recently, surfactants have been used to improve the quality of homoepitaxial as well as heteroepitaxial growth on Si and III–V substrates.[17–27].

The microscopic aspects of the mechanism by which the surfactant changes the nature of growth have been the subject of several theoretical investigations.[28–31] Irrespective of the precise mechanism, the surfactant must be able to float on the surface of the growing material, since otherwise its effect on growth would disappear beyond the first layer of deposition. The ability of different elements to float gives a natural measure of their potential to act as good surfactants. This floating ability is determined by the stable structures that the surfactant can form on the substrate and the mechanisms by which the surfactant and newly deposited atoms exchange positions.

Since group-V elements appear in general to be promising surfactants, we undertook a thorough investigation of the relative energy of various allowed reconstructions of group-V adlayers on the Si(111) substrate. The term "allowed reconstructions" refers to those structures that lead to an energetically favorable and chemically passivated surface. For group-V atoms on Si, this means that all of the group-V atoms must be threefold coordinated, while all substrate atoms must be fourfold coordinated. Several structures fit this description, including a substitutional geometry, a chain geometry and two trimer geometries, which are illustrated in Fig. 4. Although all these geometries satisfy the bonding requirements described above, there are important qualitative differences in the bonding topology, which will affect their floating ability. Specifically, in the substitutional geometry, each adsorbate atom

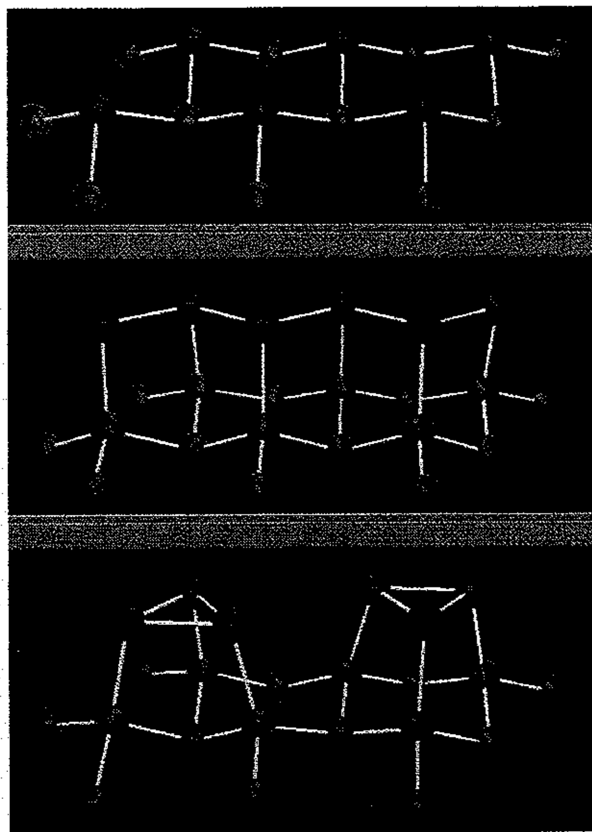

Fig. 4. Structure of the allowed reconstructions for group-V adsorbates on Si(111) (green spheres represent Si atoms and red spheres represent group-V atoms): the top panel is the substitutional geometry with each group-V atom bonded by three bonds to the substrate; the middle panel is the chain geometry; the bottom panel is the trimer geometry, with the trimer in two different possible positions. Adsorbate atoms in the chain and trimer geometries have only one covalent bond each to the substrate.

is bonded to the substrate through three strong covalent bonds, whereas in all the other geometries there is only one covalent bond between each adsorbate atom and the substrate; the other two covalent bonds of each adsorbate atom are toward other adsorbate atoms.

It is evident from this qualitative comparison that surfactants which prefer the substitutional geometry will have very poor floating ability, since three strong covalent bonds per surfactant atom need to be severed so that the surfactant layer can float during growth. In contrast, the structures where the surfactant atoms are mostly bonded to other surfactant atoms, with weaker bonding to the substrate (as in the trimer or chain geometries), are much more likely to float easily during growth. Our first-principles calculations revealed that only Sb prefers these self-bonding structures (chain or trimer) on Si(111), while As and P prefer by a large energy difference the substitutional geometry.[28] These results agree well with what is seen in experiments.[32–34] Accordingly, we predicted that As and P would be poor surfactants, while Sb would be more effective in surfactant-mediated Si homoepitaxy on Si(111).[28] These predictions were recently verified by the experimental work of Horn von Hoegen *et al.*[35]

The above theoretical prediction was admittedly based on a rather simplified picture which does not capture all the physics of the problem. Nevertheless, the fact that it was verified by experimental observation testifies to the ability of first-principles calculations to account realistically for qualitative and quantitative differences in complex physical systems.

Having demonstrated that the structure of the adsorbate layer is crucial in determining the prospects of a particular adsorbate to act as a surfactant, let us consider possible implications of this idea. We first draw analogies with the case of (100) substrates. For these substrates all group-V elements form the same reconstruction, namely a dimer reconstruction consisting of pairs of group-V atoms that bond to the substrate. In this geometry, there exists a strong bond between the two atoms in a group-V dimer, each of which is attached by two other bonds to the substrate atoms, as shown in Fig. 5. To the extent that the strong dimer bond among group-V atoms

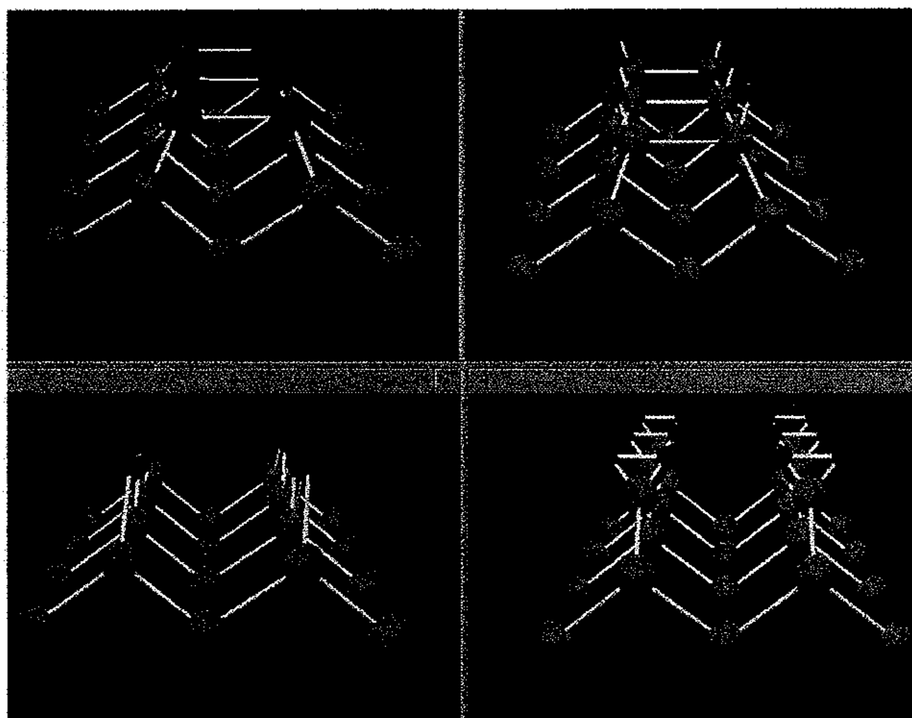

Fig. 5. Structure of the passivated Si(100) substrate with group-V (top left) or group-VI (bottom left) adsorbates and with hydrogen in the monohydride (top right) and dihydride (bottom right) phases. The green spheres represent Si substrate atoms, the large red spheres represent group-V or group-VI adsorbates, and the small red spheres represent H atoms. In the bottom-right panel the H atoms are shown bonded among themselves to draw the analogy with the group-VI passivated surface.

does not need to be broken during growth, all group-V elements should act as good surfactants on the Si(100) substrate. This seems to be the case experimentally, at least for As and Sb.[18,20] It is interesting that while As works well as a surfactant on Si(100), it is a poor surfactant on Si(111).[35] In contrast, Sb works well on both Si(100) and Si(111). The energetic comparisons discussed above provide a natural explanation for this difference between the two elements, which otherwise behave in a very similar fashion. In short, Sb forms self-bonded structures on both substrates [dimers on Si(100) and trimers or chains on Si(111)], whereas As forms a self-bonded structure only on the Si(100) substrate.

4. Use of Hydrogen as Surfactant

One of the most commonly used elements in surface passivation is hydrogen, which has also been considered as a potential surfactant (see, for example, Ref. 18). It is interesting to try to predict whether H will be an effective surfactant using the ideas developed so far. Single H atoms are very effective in saturating dangling bonds on Si and Ge surfaces. On the Si(111) surface, H can remove the complicated 7×7 reconstruction, leaving a simple 1×1 pattern in which every surface Si atom has three bonds to the substrate and one bond to a H atom situated directly above it.[36] Since the Si–H bond is particularly strong (with a bond energy of 3.5 eV compared to the Si–Si bond energy of 2.3 eV), it is reasonable to assume that Si–H bonds are not easily broken during growth. In fact, the Si–H complex resembles chemically a single group-V atom, since it has a total of five valence electrons, two of which are in a low-energy filled state (they form the strong Si–H bond) while the other three can be used to form bonds to other Si atoms. Group-V elements also have a total of five valence electrons, two of which are in a low-energy filled electronic state (the so-called lone-pair state), while the other three electrons can be used to form covalent bonds to the substrate or other group-V atoms. The passivation of the unreconstructed Si(111) surface by H implies that the Si–H complex behaves like As or P atoms (which prefer the substitutional geometry) rather than like Sb atoms (which prefer the trimer or chain geometry) on this surface. We therefore conclude that, by analogy with the results for the group-V atoms, H would *not* be a good surfactant on the Si(111) surface at monolayer coverage.

The above arguments can also be applied to the case of the Si(100) substrate. In this case, there are two possible reconstructions induced by H. The first consists of a monohydride phase, in which one H atom is attached to each surface Si atom, while the Si dimer remains intact. The second consists of a dihydride phase, in which two H atoms are attached to each Si atom, and the Si dimer bond is broken. The two structures are shown schematically in Fig. 5. The first case is similar to the structure of group-V dimers on the Si substrate, since, as we argued above, each Si–H complex resembles chemically a group-V atom. Thus, we expect that H coverage of the Si(100) substrate at the monohydride level would produce surfactant behavior similar in quality to that of As or Sb. In contrast, the dihydride phase should behave very differently. By extending the chemical argument given above, we expect that a complex consisting of a Si atom with two H atoms attached to it will behave as a group-VI atom. These atoms substitute the surface Si atoms on the Si(100) surface, forming two bonds to the substrate each. Due to their chemical valence, no other bonds need to be formed for a chemically passive, stable adsorbate layer.[37] The resulting structure is illustrated in Fig. 5. In order for such an adsorbate layer of group-VI atoms to float during growth, all of their bonds to the substrate need to be severed. This situation is very similar to the case of group-V substitutional atoms on the Si(111) surface (As or P), which do not lead to favorable surfactant behavior. We predict, then, that the dihydride phase on Si(100), acting structurally and chemically like a passivating group-VI adsorbate layer, would behave very poorly as a surfactant.

5. Conclusions

We have discussed the application of first-principles calculations to the study of diffusion and growth phenomena on semiconductor surfaces. We showed that, in the case of the Ge(111)c(2×8) reconstructed surface, these calculations were important in determining that single T_4-to-H_3 adatom hops cannot account for the observed diffusion through adatom exchanges. Rather, a complicated motion of adatoms, consisting of sequential time-correlated single hops, provides the proper description of the diffusion process, and gives the correct values for the activation energy as well as the pre-exponential factor.

In the case of surfactant-mediated growth, energy comparisons based on first-principles calculations provide the basis for predicting that chemically similar elements (P, As, Sb) can lead to very different behavior: for example, while Sb works effectively on both (100) and (111) Si substrates, As works well

only on the Si(100) substrate. These differences were explained in terms of the preferred adsorbate layer structure that the various elements assume on the substrate, which determines their ability to float during growth,[28] a necessary condition for surfactant behavior. The predicted behavior of the different group-V elements on Si(111) was subsequently verified by experiment.[35]

Finally, by drawing analogies between the structure and chemical behavior of group-V or group-VI adsorbates and that of Si–H complexes, we proposed a scenario about the possible behavior of H as a surfactant on Si(100) and Si(111) substrates: H should act as a good surfactant only in the monohydride phase of the Si(100) surface, but should be a poor surfactant in the dihydride phase of Si(100) or at monolayer coverage of the Si(111) surface.

Acknowledgment

This work was supported by the Office of Naval Research, Grant #N00014-95-1-0350.

References

1. P. Hohenberg and W. Kohn, *Phys. Rev.* **B136**, 864 (1964).
2. W. Kohn and L. J. Sham, *Phys. Rev.* **A140**, 1133 (1965).
3. A common implementation of the local density energy functional uses the results of quantum Monte Carlo calculations of D. M. Ceperley and B. J. Alder, *Phys. Rev. Lett.* **45**, 566 (1980) for the exchange-correlation functional, as parametrized by J. Perdew and A. Zunger, *Phys. Rev.* **B23**, 5048 (1981).
4. For a review of the formalism and extensive references, see: W. E. Pickett, *Computer Physics Reports* **9**, 115 (1989).
5. K. D. Brommer, M. Needels, B. E. Larson and J. D. Joannopoulos, *Phys. Rev. Lett.* **68**, 1502 (1992); I. Stich, M. C. Payne, R. D. King-Smith, J. S. Lin and L. J. Clarke, *Phys. Rev. Lett.* **68**, 1351 (1992); K. D. Brommer, M. Galvan, A. Dal Pino Jr. and J. D. Joannopoulos, *Surf. Sci.* **314**, 57 (1992); I. Stich, K. Terakura and B. E. Larson, *Phys. Rev. Lett.* **74**, 4491 (1995).
6. G. Brocks, P. J. Kelly and R. Car, *Phys. Rev. Lett.* **66**, 1729 (1991).
7. E. Kaxiras and J. Erlebacher, *Phys. Rev. Lett.* **72**, 1714 (1994).
8. N. Takeuchi, A. Selloni and E. Tosatti, *Phys. Rev. Lett.* **72**, 2227 (1994); N. Takeuchi, A. Selloni and E. Tosatti, *Phys. Rev.* **B49**, 10757 (1994).
9. A. P. Smith, J. K. Wiggs, H. Jonsson, H. Yan, L. R. Corrales, P. Nachtingall and K. D. Jordan, *J. Chem. Phys.* **102**, 1044 (1995).
10. Q.-M. Zhang, C. Roland, P. Boguslawski and J. Bernholc, *Phys. Rev. Lett.* **75**, 101 (1995).
11. For entropy estimates based on first-principles calculations, see for example: K. C. Pandey and E. Kaxiras, *Phys. Rev. Lett.* **66**, 915 (1991); E. Kaxiras and K. C. Pandey, *Phys. Rev.* **B47**, 1659 (1993).
12. E. Ganz, S. K. Theiss, I.-S. Hwang and J. Golovchenko, *Phys. Rev. Lett.* **68**, 1567 (1992); I.-S. Hwang and J. Golovchenko, *Science* **258**, 1119 (1992); I.-S. Hwang and J. Golovchenko, *Phys. Rev. Lett.* **71**, 255 (1993).
13. Y. W. Mo, J. Kleiner, M. B. Webb and M. G. Lagally, *Phys. Rev. Lett.* **67**, 1998 (1991).
14. The error bars quoted for both activation barriers represent the uncertainty due to incomplete convergence with respect to basis set size and integration in reciprocal space. We use a plane-wave basis with kinetic energy of up to 8 Ry, and a set of 16 points in the two-dimensional surface Brillouin zone. Additional errors in the calculation of the total energy of individual configurations, due to the use of the local density approximation or the pseudopotential approximation, are expected to be systematic and thus to cancel in comparisons of energy differences (which is what the activation energies represent). The calculations were performed in a 2×2 unit cell, which is simpler than the true $c(2 \times 8)$ unit cell of the surface reconstruction, but contains all the important structural features (one adatom and one rest atom).
15. G. H. Vineyard, *J. Phys. Chem. Solids* **3**, 121 (1957).
16. M. Copel, M. C. Reuter, E. Kaxiras and R. M. Tromp, *Phys. Rev. Lett.* **63**, 632 (1989).
17. R. M. Tromp and M. C. Reuter, *Phys. Rev. Lett.* **68**, 954 (1992).
18. M. Copel, M. C. Reuter, M. Horn von Hoegen and R. M. Tromp, *Phys. Rev.* **B42**, 11682 (1990); M. Horn von Hoegen, F. K. LeGoues, M. Copel, M. C. Reuter and R. M. Tromp, *Phys. Rev. Lett.* **67**, 1130 (1991); J. Falta, M. Copel, F. K. LeGoues and R. M. Tromp, *Appl. Phys. Lett.* **62**, 2962 (1993); M. Copel and R. M. Tromp, *Phys. Rev. Lett.* **72**, 1236 (1994).
19. D. J. Eaglesham, F. C. Unterwald and D. C. Jacobson, *Phys. Rev. Lett.* **70**, 966 (1993).
20. G. Meyer, B. Voigtlander and N. M. Amer, *Surf. Sci. Lett.* **274**, L541 (1992); B. Voigtlander and A. Zinner, *Surf. Sci. Lett.* **292**, L775 (1993); B. Voigtlander and A. Zinner, *J. Vac. Sci. Technol.* **A12**, 1932 (1994).
21. M. Horn von Hoegen, J. Falta, M. Copel and R. M. Tromp, *Appl. Phys. Lett.* **66**, 487 (1995).

22. G. S. Petrich, A. M. Dabiran, J. E. Macdonald and P. I. Cohen, *J. Vac. Sci. Techn.* **B9**, 2150 (1991); G. S. Petrich, A. M. Dabiran and P. I. Cohen, *Appl. Phys. Lett.* **61**, 162 (1992).
23. S. Iwanari and K. Takayanagi, *J. Cryst. Growth* **119**, 229 (1990).
24. H. Minoda, Y. Tanishiro, N. Yamamoto and K. Yagi, *Surf. Sci.* **287**, 915 (1993).
25. H. Nakahara and M. Ichikawa, *Appl. Phys. Lett.* **61**, 1531 (1992).
26. G. D. Wilk, R. E. Martinez, J. F. Chervinsky, F. Spaepen and J. A. Golovchenko, *Appl. Phys. Lett.* **65**, 866 (1994).
27. K. Fujita, S. Fukatsu, H. Yaguchi, T. Igarashi, Y. Shiraki and R. Ito, *Japan, J. Appl. Phys.* **29**, L1981 (1990); S. Fukatsu, K. Fujita, H. Yaguchi, Y. Shiraki and R. Ito, *Mat. Res. Soc. Symp. Proc.* **220**, 217 (1991); K. Fujita, S. Fukatsu, Y. Shiraki, H. Yaguchi, Y. Shiraki and R. Ito, *Appl. Phys. Lett.* **61**, 210 (1992); N. Usami, S. Fukatsu and Y. Shiraki, *Appl. Phys. Lett.* **63**, 388 (1993); Y. Shiraki, S. Fukatsu, K. Fujita and T. Usami, *Mat. Res. Soc. Symp. Proc.* **318**, 191 (1994); Y. Shiraki and S. Fukatsu, *Semicond. Sci. Technol.* **9**, 2017 (1994).
28. E. Kaxiras, *Europhys. Lett.* **21**, 685 (1993); E. Kaxiras, *Materials Science and Engineering* **B30**, 175 (1995).
29. B. D. Yu and A. Oshiyama, *Phys. Rev. Lett.* **71**, 585 (1993); B. D. Yu and A. Oshiyama, *Phys. Rev. Lett.* **72**, 3190 (1994).
30. Z. Zhang and M. G. Lagally, *Phys. Rev. Lett.* **72**, 693 (1994).
31. D. Kandel and E. Kaxiras, *Phys. Rev. Lett.* **75**, 2742 (1995).
32. F. Boszo and Ph. Avouris, *Phys. Rev.* **B43**, 1847 (1991).
33. R. S. Becker, B. S. Swartzentruber, J. S. Vickers, M. S. Hybertsen and S. G. Louie, *Phys. Rev. Lett.* **60**, 116 (1988); M. Copel, R. M. Tromp and U. K. Köhler, *Phys. Rev.* **B37**, 10756 (1988); M. Copel and R. M. Tromp, *Phys. Rev.* **B37**, 2766 (1988).
34. P. Martensson, G. Meyer, N. M. Amer, E. Kaxiras and K. C. Pandey, *Phys. Rev.* **B42**, 7230 (1990).
35. M. Horn von Hoegen, J. Falta, M. Copel and R. M. Tromp, *Appl. Phys. Lett.* **66**, 487 (1995).
36. E. Kaxiras and J. D. Joannopoulos, *Phys. Rev.* **B37**, 8842 (1988).
37. E. Kaxiras, *Phys. Rev.* **B43**, 6824 (1991); *Mat. Res. Soc. Symp. Proc.* **193**, 143 (1990).